Measurement of Neutral Densities at the Outer Midplane in DIII-D

R.J. Colchin, N.H. Brooks,[1] L.W. Owen, R.Maingi, R.C. Isler
T.N. Carlstrom[1] and R.J. Groebner[1]

Oak Ridge National Laboratory, Oak Ridge, Tennessee

[1]General Atomics, P.O. Box 85608, San Diego, CA 92186-5608

Initial measurements of neutral densities near the separatrix at the outer midplane of DIII-D are described. Measurements of the neutral density near the X-point were reported previously [1–3]. The current measurements, coupled with code calculations [4], are focused on the role that neutrals play in the L-H transition, and in plasma fueling. The midplane measurements employ a new array of eight calibrated D_α tangentially-viewing monitors which span the outer separatrix just below the outer midplane in DIII-D. D_α intensities from these detectors, coupled with Thomson scattering measurements of the electron temperature and density, provide the information necessary to determine radial profiles of neutral density and ionization rates. Preliminary results show separatrix neutral densities $n_o \sim 10^9$–10^{10} atoms/cm^3 and $n_o/n_e \sim 10^{-4}$–10^{-3}. The diagnostic, method of data analysis, and preliminary results are described in this paper.

Midplane Filterscope

The new fan of eight tangentially-viewing monitors shown in Fig. 1 lies 20 cm below the outer midplane of DIII-D. At the tangency point of each viewing chord, the diameter of the acceptance cones is 1 cm, and the chord spacing is 1 cm, so that the acceptance cones just "touch." As a shield against reflected plasma light, the acceptance cones are incident on razor-blade viewing dumps, with collimation provided by a 1.6 cm diameter hole bored in the overlying carbon tile. Baffling of the dump gives a plasma light rejection of over 20:1 relative to the signal on the brightest chord. This rejection of extraneous plasma light is key to successful measurements.

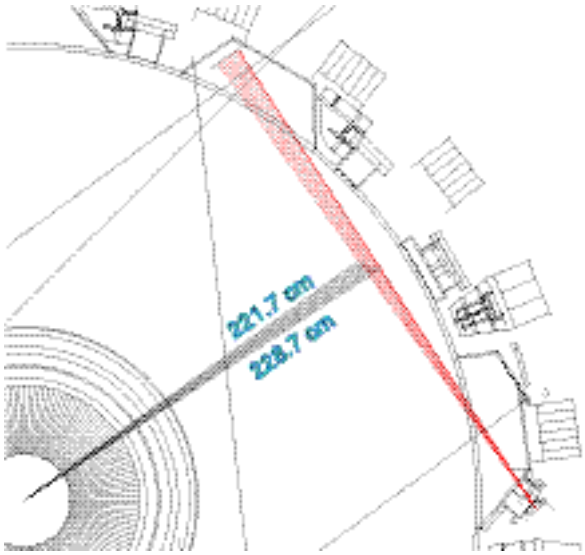

Fig. 1. Midplane filterscope, showing a fan of eight viewchords and their tangency radii, which range from 221.7 to 228.7 cm.

Light from each chord is focused onto an optical fiberguide which conveys the light to detectors located outside the Experimental Hall. After a three-way division in a fiber splitter, the light is imaged through notch filters (D_α, C III, and visible bremsstrahlung passbands) onto photomultiplier tubes in an apparatus called a Filtersope. The signals are absolutely calibrated by means of an integrating light source (Optronics Laboratory, Unisource 6000) placed inside the DIII-D vacuum vessel. Small nonlinearities in the gain of the photomultiplier tubes with light intensity have been corrected.

Inversion of the Data

The column-integrated brightness [photons/cm^2-s-str] must be inverted to determine the emission [photons/cm^3-s] profile. Straight forward matrix inversions of the data can fail because extreme accuracy is required of the data, i.e. the problem is ill posed. To invert the data, an "onion peeling" model is invoked. Toroidal plasma symmetry is assumed and the horizontal cross section of the plasma is divided into eight rings. The inner seven rings are 1 cm wide and centered at the tangency radii of the respective viewchords. The D_α intensity is assumed constant inside each ring, representing an average over the width of the ring. The outer ring is thicker than the other rings and extends to the outer wall at 237.5 cm. It contains only the outer viewing chord.

The length of a viewchord segment within each ring is determined by summing the volume-weighted average differential lengths $\Delta\ell_n = \Delta x(\Delta V_n / V_x)$ along the length of the chord, where Δx is the differential length along the chord, V_x is the volume inside the acceptance cone of length Δx, and ΔV_n is the portion of this volume in ring n. The lengths of the segments containing the tangency point are approximately 30 cm, or approximately 20% of the total chordal length. The length of the outer chord is 126.6 cm. Since the radial variation of light along the outer chord is not known, it is impossible to assign an intensity-weighted radius to this ring. This chord is used only to subtract a boundary brightness from the other chords. This procedure is valid only if the brightness of the outer chord is small compared with the signal on all other chords.

The contribution from each ring to the column-integrated brightness is unfolded by subtracting the signals from all outer chords, i.e., "peeling" the onion. The emision of each central chord segment is then determined by dividing the brightness (photons/ cm^2-s-str) by the central chord length and multiplying by the solid angle. The brightness and emission for a typical L-mode plasma are show in Fig. 2. The line average density was 2.5 x 10^{19} m^{-3}, I_p = 1.1 MA, B_T = -2.1 T, 2.4 MW of neutral beam power was applied, and the D_α data were averaged over 10 ms (10 digital samples). This upper single null discharge had the ion grad-B drift downward, raising the L-H transition power threshold.

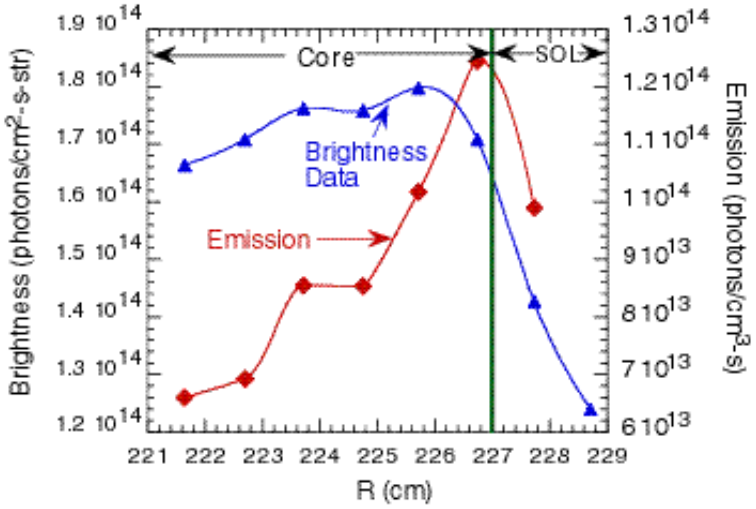

Fig. 2. Brightness and emission for an L-mode discharge, shot #102028 at 1400 ms.

Initial Results

The neutral density n_0 is related to the emission by the relation $n_0 = I / n_e\langle\sigma v\rangle_{exc}$, where I is the D_α emission, n_e is the electron density, and $\langle\sigma v(T_e, n_e)\rangle_{exc}$ is the electron excitation rate coefficient [5]. This coefficient is a sensitive function of the electron temperature and density, which are measured by Thomson scattering and mapped poloidally along flux surfaces to the tangency point locations of the D_α viewchords.

Plotted in Fig. 3 is the neutral density profile calculated from the D_α intensities shown in Fig. 2. The scale of the horizontal axis is plotted in normalized flux surface coordinates and shows data extending into Ψ_N = 0.85. Thomson scattering data for n_e and T_e were averaged over 16 laser pulses, and vertical error bars are estimated from Thomson scattering photon

statistics. Systematic errors due to D_α calibration and data inversion have not been quantified. Horizontal bars represent the width of each of the "onion" rings in which the intensity is assumed constant.

Figure 4 shows the neutral densities from three different times during the same shot, as a function of major radius. The data of Fig. 3 are shown as the middle curve in Fig. 4. The top curve is data during the ohmic portion of the discharge, before neutral injection. The H-mode (lower curve) data were averaged between ELMs. The inversion process failed at the inner four viewchords.

From the intensity data, the ionization rate can be deduced using cross section data from the ADAS* data base. Figure 5 shows the ionization rates corresponding to the neutral densities of Fig. 4. Note that ionization rates peak inside the separatrix in Fig. 5.

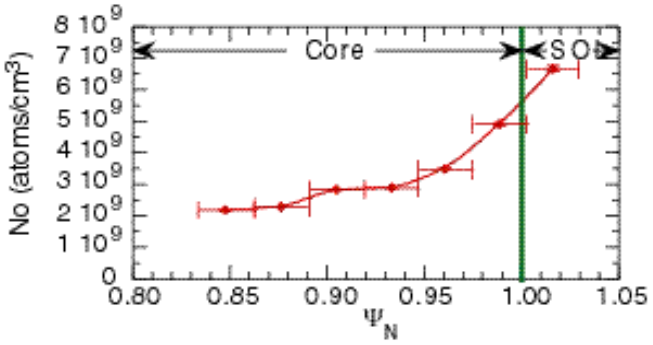

Fig. 3. L-mode, neutral density profile. The horizontal axis is in normalized flux coordinates. Vertical error bars (small) are the result of Thomson scattering photon statistics. Horizontal bars represent the size of the "onion" rings.

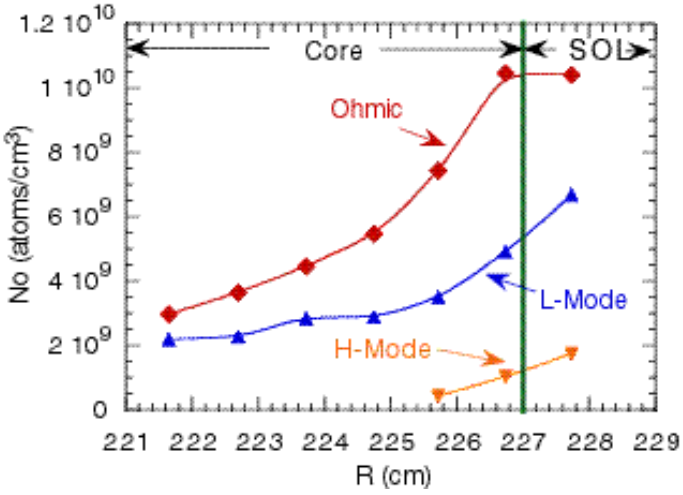

Fig. 4. Neutral densities measured in discharge #102028 at 1000 ms (ohmic), at 1400 ms (L-mode), and at 1750 ms (H-mode).

Discussion of Data

The neutral densities measured at the separatrix (Fig. 4) are in the range of 10^9–10^{10} atoms/cm^3. This is an order of magnitude lower than the densities at the X-point reported previously [2]. Detailed comparisons with modeling calculations have not yet been performed, but simple slab model calculations suggest that steep slope of the ohmic curve (Fig. 4, upper curve) at larger radii can be explained by attenuation of thermal molecular deuterium from the vacuum vessel walls. At smaller radii, however, the slope of the neutral density curves show a slower rate of decline than might be expected from one-dimensional calculations. There are two possible explanations: either calibration errors coupled with the inversion process lead to the small slope or there are contributions from non-thermal neutrals. Initial (and on-going) modeling efforts using a Monte Carlo code have shown approximate fits to the brightness data.

Similar recent measurements of neutrals have been carried out by Baird [6] in ASDEX Upgrade and by Boivin [7] in Alcator C-mod. Measurements at the midplane of Alcator C-Mod using Lyman alpha radiation yielded separatrix neutral densities of order 10^{11} atoms/cm^{-3}, and peaks in the ionization rate that shift to inside the separatrix in the H-mode. At ratios of $n_o/n_e \sim 10^{-4}$, neutrals are found to dominate the parallel ion flow velocity [7].

*The originating developer of ADAS is the JET Joint Undertaking.

Neutral density measurements [8] at the X-point in DIII-D show no decline in the neutral density upon transition to the H-mode. Figure 4 shows a decline in the neutral density at the outer midplane following the application on 2.4 MW of neutral beam power (middle curve) and an even larger drop after the H-mode transition. Since neutrals act to damp the rotational momentum increase during the L-H transition, these data suggest that the beam power facilitates the transition by lowering the neutral density near the midplane. Calculations are needed to quantify the neutrals momentum damping relative to other damping mechanisms in the midplane area.

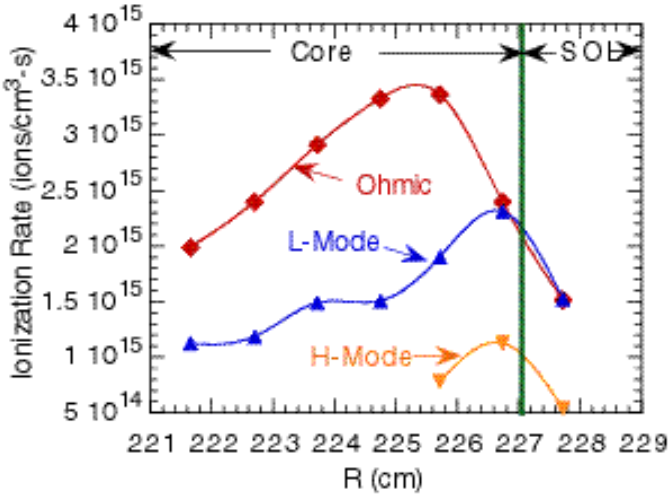

Fig. 5. Ionization rates for discharge #102028 at 1000 ms (ohmic), at 1400 ms (L-mode), and at 1750 ms (H-mode).

Acknowledgment

This is a report of work supported by the U.S. Department of Energy under Contract Nos. DE-AC03-99ER54463 and DE-AC05-00OR22757.

References

[1] R.J. Colchin *et al.*, in Controlled Fusion and Plasma Physics, (Proc. 25th Euro. Conf. Praha, 1998) Vol. 22C, (European Physical Society, Geneva, 1999) p. 818.

[2] R.J. Colchin *et al.*, Nucl. Fusion **40**, (2000) 175.

[3] R., Maingi *et al*, in Controlled Fusion and Plasma Physics, (Proc. 26th Euro. Conf. Maastricht, 1999) Vol. 23J, (European Physical Society, Geneva, 1999) p. 329.

[4] L.W. Owen, *et al*., Plasma Phys. Contr. Fusion **40** (1998) 717.

[5] R.K Janev and J.J Smith, *Atomic and Plasma-Material Interaction Data for Fusion*, Supplement to Nucl. Fusion (International Atomic Energy Agency, Vienna, 1993) Vol. 4, p. 1.

[6] A. Baird, *et al*., in Controlled Fusion and Plasma Physics, (Proc. 25th Euro. Conf. Praha, 1998) Vol. 22C (European Physical Society, Geneva, 1998) p. 1514.

[7] R.L. Boivin, *et al.*, Phys. Plasmas **5** (2000) 1919.

[8] L.W. Owen, *et al.*, "Origins and Distributions of Core Fueling in the DIII-D Tokamak," submitted to J. of Nucl. Materials.